Available online at website: https://journal.bcrec.id/index.php/bcrec

Bulletin of Chemical Reaction Engineering & Catalysis, 22 (1) 2027, 55-68

Original Research Article

Immobilization of Purified α-Amylase from *Aspergillus fumigatus* on a Chitosan–Silica Gel 60 Hybrid: Enhanced Thermal Stability and Reusability

Santalum Alba[1], Yandri Yandri[2,*], Tati Suhartati[2], Bambang Irawan[3], Stevenson Waruwu[4]

[1]*Department of Cosmetic Engineering, Faculty of Industrial Technology, Institut Teknologi Sumatera, South Lampung 35365, Indonesia.*
[2]*Department of Chemistry, Faculty of Mathematics and Natural Sciences, University of Lampung, Bandar Lampung 35145, Indonesia.*
[3]*Department of Biology, Faculty of Mathematics and Natural Sciences, University of Lampung, Bandar Lampung 35145, Indonesia.*
[4]*Postgraduate Program in Chemistry, Faculty of Mathematics and Natural Sciences, University of Lampung, Bandar Lampung 35145, Indonesia.*

Received: 2nd October 2026; Revised: 2nd November 2026; Accepted: 2nd November 2026
Available online: 6th November 2026; Published regularly: April 2027

Abstract

Free α-amylase is inactivated at high temperatures and cannot be recovered after starch hydrolysis, which limits its industrial use. Silica is robust but leaches enzymes, whereas chitosan binds enzymes strongly but dissolves in acid, so a hybrid is needed; however, a chitosan–silica gel 60 hybrid has not been reported for *Aspergillus fumigatus* α-amylase. This study compared the catalytic properties, thermal inactivation kinetics, and reusability of *A. fumigatus* α-amylase immobilized on silica gel 60, chitosan, and the hybrid. The enzyme was purified by (30–90)% ammonium sulfate fractionation and dialysis, increasing its specific activity from 702.23 to 3449.43 U/mg. The hybrid, synthesized with glutaraldehyde as a cross-linker, showed the FT-IR bands of both components with wavenumber shifts, indicating their interaction. The enzyme was immobilized by physical adsorption at an optimum binding pH of 5.0 on all matrices. Immobilization raised the optimum temperature from 50 to 55 °C, increased K_M from 3.48 to 4.62–5.80 mg.mL^{-1}, and decreased V_{max} from 12.97 to 2.72–3.73 μmol.mL^{-1}.min^{-1}. After 80 min at 60 °C, the purified enzyme retained 24.8% of its activity, whereas the enzyme immobilized on silica gel 60, chitosan, and the hybrid retained 77.3, 55.1, and 81.1%, respectively. The enzyme–hybrid had the longest half-life (260.85 min; a 6.5-fold increase), the highest free energy of inactivation (109.62 kJ.mol^{-1}), and the highest residual activity after six reuse cycles (57%). The chitosan–silica gel 60 hybrid is a more effective support than either of its components for stabilizing and reusing α-amylase.

Copyright © 2027 by Authors, Published by BCREC Publishing Group. This is an open access article under the CC BY-SA License (https://creativecommons.org/licenses/by-sa/4.0).

Keywords: α-Amylase; *Aspergillus fumigatus*; chitosan–silica gel hybrid; immobilization; thermal stability

How to Cite: Alba, S., Yandri, Y., Suhartati, T., Irawan, B., Waruwu, S. (2027). Immobilization of Purified α-Amylase from *Aspergillus fumigatus* on a Chitosan–Silica Gel 60 Hybrid: Enhanced Thermal Stability and Reusability. *Bulletin of Chemical Reaction Engineering & Catalysis*, 22 (1), 55-68. (DOI: 10.9767/bcrec.20874)

Permalink/DOI: https://doi.org/10.9767/bcrec.20874

Supporting Information (SI): https://journal.bcrec.id/index.php/bcrec/article/downloadSuppFile/20874/6674

1. Introduction

α-Amylase (EC 3.2.1.1) catalyzes the hydrolysis of the α-1,4-glycosidic bonds of starch and is one of the most widely used industrial enzymes, with applications in starch processing and in the food, textile, detergent, and bioethanol industries [1,2]. The fungus *Aspergillus fumigatus* is one source of α-amylase, which can be produced by fermentation with corn starch as an inducer [3,4]. However, the free enzyme is generally unstable at elevated temperatures and difficult to separate from the reaction mixture, so it cannot be reused; this raises the biocatalyst cost per unit of product and complicates downstream processing [5,6].

Immobilization on a solid support converts the enzyme into a heterogeneous biocatalyst that

* Corresponding Author.
Email: yandri.as@fmipa.unila.ac.id (Y. Yandri)

can be recovered and reused in batch or continuous reactors, and binding to the support can also rigidify the enzyme structure and thereby improve its stability [5,7]. Immobilization by physical adsorption is simple and does not require a cross-linking agent to attach the enzyme; the enzyme–support interaction is governed by electrostatic effects and hydrogen bonding [8]. Binding to a matrix can make the enzyme more rigid and thus more resistant to heat-induced conformational changes [9,10]. Such improvements have been reported for *A. fumigatus* α-amylase adsorbed on bentonite [10] and chitin–bentonite [4], and for α-amylases from other sources immobilized on chitosan–magnetic nanoparticles [11], a chitosan–TiO_2 nanocomposite [9], and a polyaniline magnetic nanocomposite [12]. On the chitosan–magnetic and polyaniline magnetic supports, immobilization improved the thermal stability and reusability of the enzyme but increased its apparent K_M, indicating a lower apparent affinity for starch [11,12].

Silica and chitosan are two widely studied immobilization supports with complementary properties. Porous silicas are mechanically and thermally robust and carry surface silanol groups that can bind enzymes, but physically adsorbed enzymes may leach from the silica surface [13]; silica-based carriers have also been applied to amylolytic enzymes for starch hydrolysis [14]. Silica gel 60, for example, is insoluble in water at pH of 4–8. Chitosan, in contrast, is a biocompatible polysaccharide whose amino and hydroxyl groups can interact with enzymes, but it dissolves to form a gel at acidic pH [15]. Combining the two materials into a hybrid could therefore merge their advantages, namely low solubility at acidic pH and more extensive interaction with the enzyme. Chitosan–silica supports have been used to immobilize laccase [16] and pepsin [17], the latter showing improved stability at high temperature and reusability for 8–10 cycles, and chitosan-based hybrids with zeolite and bentonite have improved the thermal stability of *A. fumigatus* α-amylase [18,19].

Among these hybrids, the bentonite/chitosan matrix increased the half-life of *A. fumigatus* α-amylase at 60 °C 4.44-fold and retained 47.61% of the initial activity after six reuse cycles [19]. To the best of our knowledge, however, a hybrid of chitosan with silica gel 60 has not been evaluated as a support for this enzyme. In addition, the contribution of hybridization can only be distinguished from that of each component when the hybrid and its individual components are compared under identical conditions, in terms of both the apparent kinetic parameters and the thermal inactivation kinetics and thermodynamics of the immobilized biocatalyst.

The novelty of this work is therefore twofold. First, to the best of our knowledge, a chitosan–silica gel 60 hybrid is reported here for the first time as a support for α-amylase, since chitosan–silica supports have so far been applied only to laccase and pepsin [16,17], and new FT-IR evidence (Section 3.4) is provided that the hybrid is a hydrogen-bonded and electrostatically linked chitosan–silica network rather than a simple physical mixture of its components. Second, because the hybrid, silica gel 60, and chitosan were immobilized and characterized in parallel under identical conditions, the contribution of hybridization beyond that of either component is quantified directly: the hybrid gave the highest thermal stability (6.5-fold increase in half-life; 81.1% residual activity after 80 min) and the highest reusability (57% residual activity after six cycles) among the three matrices, and a larger half-life increase than the chitin–bentonite, bentonite, zeolite/chitosan, and bentonite/chitosan supports previously tested for *A. fumigatus* α-amylase [4,10,18,19]. This gain in stability is accompanied by a lower catalytic efficiency, whose consequence for productivity is analyzed quantitatively in Section 3.7. Together, these results define what the chitosan–silica gel 60 hybrid contributes, and what it costs, relative to its components and to earlier hybrid supports for this enzyme.

Therefore, this study aimed to purify α-amylase from *A. fumigatus*, to synthesize and characterize a chitosan–silica gel 60 hybrid, and to compare the enzyme immobilized on silica gel 60, chitosan, and the hybrid with the purified enzyme. The parameters compared were the binding pH, optimum temperature, kinetic parameters (K_M and V_{max}), thermal inactivation rate constant, half-life, free energy change of inactivation, and reusability.

2. Materials and Methods

2.1. Materials and Equipment

A local isolate of *A. fumigatus* was obtained from the Microbiology Laboratory, Department of Biology, University of Lampung. The main materials were silica gel 60 (0.2–0.5 mm; Merck); medium-molecular-weight chitosan (190–310 kDa; degree of deacetylation 75–85%), 25% glutaraldehyde, and 3,5-dinitrosalicylic acid (Sigma-Aldrich); soluble potato starch (Loba Chemie); corn starch (Maizenaku); and potato dextrose agar (PDA) and peptone (HiMedia). Most other chemicals were obtained from Merck. Absorbance was measured with a UV-Vis spectrophotometer (Thermo Genesys 150), and infrared spectra were recorded with an FT-IR spectrophotometer (Shimadzu IRSpirit).

Copyright © 2027, ISSN 1978-2993

2.2. Production of the Crude α-Amylase Extract

The agar slant medium was prepared from 0.1 g of corn starch and 3.9 g of PDA in 100 mL of distilled water [3]. The inoculum and fermentation media had the same composition (% w/v): KH_2PO_4 2.0; $(NH_4)_2SO_4$ 1.40; corn starch 0.75; peptone 0.75; urea 0.30; $CaCl_2$ 0.30; $MgSO_4$ 0.30; $FeSO_4 \cdot 7H_2O$ 0.005; $CoCl_2$ 0.002; and $ZnSO_4 \cdot 7H_2O$ 0.0014 [20]. The inoculum medium was prepared in 100 mL of distilled water, whereas the fermentation medium was prepared in seven 1000 mL Erlenmeyer flasks, each containing 500 mL of 0.05 M phosphate buffer, pH 6.5. All media were sterilized at 121 °C and 1 atm for 15 min.

The *A. fumigatus* isolate was grown on the agar slant for approximately 5 days [3]. Three loopfuls of the isolate were then aseptically inoculated into the inoculum medium and incubated in a shaker incubator at 125 rpm and room temperature for 24 h. The inoculum (2%, v/v) was transferred to each fermentation medium and incubated under the same conditions for 112 h, the optimum fermentation time [4]. The fermentation broth (3500 mL in total) was centrifuged at 2–4 °C and 5000 rpm for 15–20 min, and the supernatant was filtered and used as the crude enzyme extract.

2.3. Enzyme Purification

The crude extract was fractionated stepwise with ammonium sulfate at saturations of (0–15), (15–30), (30–45), (45–60), (60–75), and (75–90)% [21]. At each step, ammonium sulfate was added slowly to 100 mL of crude extract or to the filtrate from the previous step with gentle stirring at 2–4 °C; the mixture was centrifuged (2–4 °C, 5000 rpm, 15–20 min), and the precipitate was dissolved in 0.025 M phosphate buffer, pH of 6.5 (1–2 times the precipitate volume). Based on the specific activity profile of the fractions, each 1000 mL of crude extract was subsequently fractionated into two fractions, (0–30) and (30–90)%, to increase enzyme recovery, and the precipitate was dissolved in 25 mL of 0.025 M phosphate buffer, pH 6.5 [4].

A 20 mL portion of the (30–90)% fraction was dialyzed in a cellophane bag against 0.01 M phosphate buffer, pH of 6.5, at 2–4 °C for 24 h with magnetic stirring, and the buffer was replaced every 4–6 h. Unit activity and protein content were determined for the crude extract, each fraction, and the dialyzed enzyme.

2.4. Determination of Unit Activity and Protein Content

Enzyme activity during production and purification was determined by the Fuwa method [21,22]. A mixture of 0.25 mL of enzyme and 0.25 mL of 0.1% starch solution was incubated at 60 °C for 10 min, and the reaction was stopped with 0.25 mL of 1 N HCl. After the addition of 0.25 mL of iodine reagent and 4.0 mL of distilled water, the absorbance was measured at 600 nm. For the control, HCl was added before incubation and starch afterward. The unit activity (*AU*) was calculated using Equation (1):

$$AU = \left[\frac{A_{\text{control}} - A_{\text{sample}}}{A_{\text{control}}}\right] \times \frac{1}{V} \times DF \quad (1)$$

where A_{control} and A_{sample} are the absorbances of the control and the sample, V is the enzyme volume (0.25 mL), and DF is the dilution factor.

At the characterization stage, enzyme activity was determined by the Mandels method [23], based on the reducing sugar formed. A mixture of 0.25 mL of enzyme and 0.25 mL of 0.1% starch solution was incubated at 60 °C for 30 min (for the control, starch was added after incubation); 1 mL of 3,5-dinitrosalicylic acid (DNS) reagent was then added, and the mixture was boiled for 10 min, cooled, and diluted with 1.5 mL of distilled water. Absorbance was measured at 510 nm against a DNS–distilled water blank (1:2), and the glucose concentration was determined from a glucose standard curve. Unit activity was calculated using Equation (2):

$$AU = \frac{[(A_{\text{sample}} - A_{\text{control}}) - b]}{a} \times \frac{1}{V} \times \frac{1}{t} \times \frac{1000 \times DF}{M_{\text{r}}} \quad (2)$$

where a and b are the slope and intercept of the glucose standard curve, t is the incubation time (30 min), and M_{r} is the relative molecular mass of glucose (180 g.mol^{-1}).

Protein content was determined by the Lowry method with bovine serum albumin (BSA; 20–140 ppm) as the standard [21,24]. A 0.1 mL enzyme sample in 0.9 mL of distilled water was reacted with 5 mL of alkaline copper reagent (2% Na_2CO_3 in 0.1 N NaOH with $CuSO_4 \cdot 5H_2O$ and Na/K tartrate) for 10 min and then with 0.5 mL of Folin–Ciocalteu reagent (1:1) for 30 min, and the absorbance was measured at 750 nm.

2.5. Synthesis and Characterization of the Chitosan–Silica Gel 60 Hybrid

Chitosan (7 g) was suspended in 500 mL of 1.0 M acetic acid and stirred for 24 h at 30 °C. After the addition of 5 mL of 1% glutaraldehyde as a cross-linker and 7 g of silica gel 60, the mixture was stirred for 4 h at 60 °C. The resulting hybrid was washed with distilled water by repeated centrifugation until the washings were neutral, dried in an oven at 60 °C, cooled in a desiccator, and ground into a fine powder [16,25]. FT-IR spectra of chitosan, silica gel 60, and the hybrid (0.5 g of powder each) were recorded over 4000–400 cm^{-1} [26]. Glutaraldehyde was used at this synthesis stage to cross-link chitosan and anchor it onto silica gel 60. Residual glutaraldehyde was

Copyright © 2027, ISSN 1978-2993

expected to be removed by the repeated washing, so the enzyme was not intentionally exposed to a cross-linker during the subsequent immobilization (Section 2.6).

2.6. Enzyme Immobilization

The dialyzed enzyme was immobilized by physical adsorption on silica gel 60, chitosan, and the hybrid [10,27]. To determine the binding buffer pH, 0.20 g of each matrix was rinsed three to four times with 0.1 M phosphate buffer at pH 4.0–8.0 (4.0–8.5 for silica gel 60) in 0.5 pH-unit steps, the buffer being removed by centrifugation. The matrix was then incubated with 0.5 mL of enzyme and 0.5 mL of the same buffer at 4 °C for 30 min and centrifuged, and 0.25 mL of the supernatant was taken as the control. The immobilized enzyme was reacted with 0.75 mL of starch substrate at 60 °C for 30 min, and its activity was determined by the Mandels method. The pH giving the highest activity was selected as the binding pH.

Immobilization was performed by equilibrating 0.20 g of matrix with the binding buffer through repeated buffer exchange and centrifugation, followed by incubation with 0.5 mL of enzyme and 0.5 mL of binding buffer at 4 °C for 30 min. After centrifugation, 0.25 mL of the supernatant was taken as the control for the Mandels assay. The immobilized enzyme was then reacted with 0.75 mL of starch substrate at the optimum temperature for 30 min and separated by centrifugation, and 0.5 mL of the supernatant was assayed as the sample by the Mandels method.

The binding pH is defined as the pH of the buffer in which the matrix was equilibrated before the enzyme was added; it was selected for the highest activity of the enzyme retained on the matrix (Section 3.5) and is therefore an apparent property of the adsorption step. It is not necessarily identical to the pH of highest catalytic activity of the free enzyme in solution (pH 5.5, Section 3.2), because adsorption onto a charged solid surface and the intrinsic pH dependence of catalysis are different processes. The starch substrate was prepared in the same buffer as that used for binding and was added directly to the matrix, without further buffer exchange, so the bound enzyme was not subjected to a change of pH between the binding and the catalytic steps. Detachment of the enzyme caused by a pH shift is therefore not expected under the present protocol; the gradual loss of activity during reuse (Section 3.10) occurred at constant pH and is attributed to desorption during repeated washing.

2.7. Optimum pH, Optimum Temperature, and Kinetic Parameters

The purified enzyme used for characterization was the dialyzed enzyme diluted 10-fold. Its optimum pH was determined over pH 4.0–8.5 (0.5 pH-unit intervals) by the Mandels assay. The optimum temperatures of the purified and immobilized enzymes were determined by the Mandels assay at 45–80 °C (5 °C intervals) for 30 min [10]. The kinetic parameters K_M and V_{max} were determined at starch concentrations of 1.0, 2.0, 4.0, 6.0, and 8.0 mg.mL^{-1} at the respective optimum temperatures [28] and calculated from Lineweaver–Burk plots of $1/V$ versus $1/[S]$ (Equation (3)):

$$\frac{1}{V} = \frac{K_M}{V_{max}} \times \frac{1}{[S]} + \frac{1}{V_{max}} \quad (3)$$

where V is the reaction rate and [S] is the starch concentration.

2.8. Thermal Stability and Thermal Inactivation Kinetics

Thermal stability was determined from the residual activity after heating the enzyme at 60 °C for 0–80 min (10 min intervals), with activity assayed by the Mandels method at the respective optimum temperature [11,12]. The thermal inactivation rate constant (k_i) was obtained from the slope of $\ln(E_i/E_0)$ versus time according to first-order kinetics (Equation (4)), and the half-life ($t_{1/2}$) and the free energy change of inactivation (ΔG_i) were calculated using Equations (5) and (6), respectively.

$$\ln\left(\frac{E_i}{E_0}\right) = -k_i t \quad (4)$$

$$t_{1/2} = \frac{\ln 2}{k_i} \quad (5)$$

$$\Delta G_i = -RT \ln\left(\frac{k_i h}{k_B T}\right) \quad (6)$$

where E_0 and E_i are the enzyme activities before and after heating for time t, R is the gas constant, T is the inactivation temperature (333 K), h is Planck's constant, k_B is the Boltzmann constant, and k_i is expressed in s^{-1} in Equation (6). The stability increase was expressed as the ratio of the $t_{1/2}$ of the immobilized enzyme to that of the purified enzyme.

2.9. Reusability

Reusability was tested by washing the used immobilized enzyme with the initial buffer (by centrifugation) and then reacting it again with 0.75 mL of fresh substrate; 0.25 mL of the wash supernatant was taken as the control. This cycle was repeated up to six times [25], and the activity in the first cycle was set as 100%.

Copyright © 2027, ISSN 1978-2993

3. Results and Discussion

3.1. Production and Purification of α-Amylase

The crude enzyme extract obtained from *A. fumigatus* fermentation had a unit activity of 53.76 $U.mL^{-1}$, a protein content of 0.153 $mg.mL^{-1}$, and a specific activity of 702.23 U/mg. Ammonium sulfate fractionation was used to precipitate the enzyme stepwise, separating it from other proteins and from the aqueous solvent. In the fractionation profile, the highest specific activity, 1572.64 $U.mg^{-1}$, was obtained in the (30–45)% fraction, whereas the other fractions gave much lower specific activities (Figure 1). Based on this result, large-scale fractionation used two ranges, (0–30) and (30–90)%, to maximize enzyme recovery, because the enzyme in this range still had high catalytic activity.

The (30–90)% fraction had a higher specific activity than the (0–30)% fraction (Figure 2) and was selected for dialysis. The specific activity of the (30–90)% fraction was 2520.91 $U.mg^{-1}$, corresponding to a 3.6-fold purification relative to the crude extract (Table 1). This increase resulted from the precipitation of other proteins in the first (0–30)% fraction and from the separation of the precipitated enzyme from water and soluble impurities. The extract volume also decreased from 1000 mL to 25 mL, a 40-fold concentration, which increased the unit activity of the enzyme [29].

Dialysis for 24 h against 0.01 M phosphate buffer, pH of 6.5, was intended to remove salt ions and other inorganic ions from the enzyme. The dialyzed enzyme had a specific activity of 3449.43 U/mg, a 4.9-fold purification relative to the crude extract (Table 1). This increase in purity was due to the diffusion of salt ions out through the cellophane membrane, while the high-molecular-weight enzyme was retained inside the bag. The enzyme volume tripled, from 20 mL to 60 mL, because of the osmotic influx of water from the dialysis buffer, which lowered the unit activity of the enzyme [30].

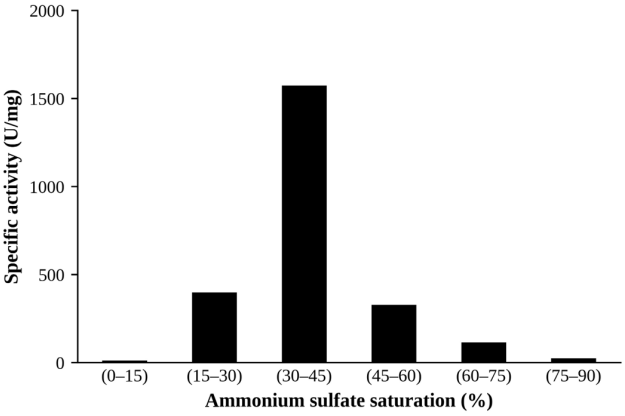


Figure 1. Relationship between ammonium sulfate saturation and the specific activity of α-amylase from *A. fumigatus*.

3.2. Optimum pH of the Purified Enzyme

The purified enzyme showed optimum activity at pH of 5.5 (Figure 3). Activity decreased considerably as the pH became more alkaline, indicating that the enzyme works optimally under slightly acidic conditions.

3.3. Synthesis of the Chitosan–Silica Gel 60 Hybrid

The chitosan used was a fine, yellowish-white powder. Its molecular weight and degree of deacetylation (Section 2.1) are important because they affect chitosan solubility: the higher the molecular weight and the lower the degree of deacetylation, the lower the solubility of chitosan. Silica gel 60 is a fine white powder that is insoluble in water at pH of 4–8 and is therefore suitable as an immobilization matrix. Synthesis from 7 g of silica gel 60 and 7 g of chitosan with glutaraldehyde as a cross-linker yielded 9.9 g of

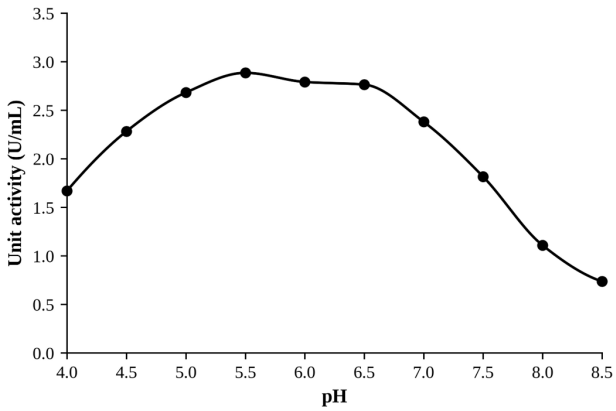


Figure 3. Unit activity of purified α-amylase from *A. fumigatus* at various pH values.

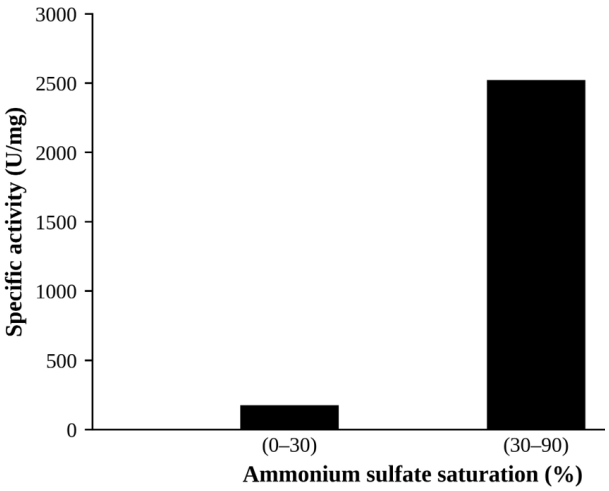


Figure 2. Relationship between ammonium sulfate saturation of (0–30)% and (30–90)% and the specific activity of α-amylase from *A. fumigatus*.

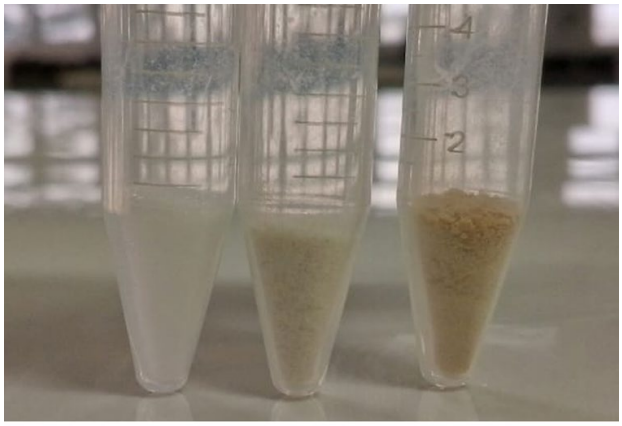
Copyright © 2027, ISSN 1978-2993

hybrid as a fine, yellowish-white powder that was easily separated from the buffer solution by centrifugation (Figure 4).

Glutaraldehyde was included in the synthesis following established chitosan–silica protocols [16,17,25]. Its two aldehyde groups can react with the amino groups of chitosan to form imine linkages that cross-link the chitosan chains and tie them to the silica surface, which is expected to limit the dissolution of chitosan at acidic pH; the shifts of the amide I and N–H bands (Section 3.4) are consistent with such linkages. A hybrid prepared without a cross-linker was not synthesized in this study. The extent of hybridization, and the immobilization results, without a cross-linker are therefore not known, and this comparison is identified as a limitation of the present work and as a direction for future work.

3.4. FT-IR Analysis

The FT-IR spectra of silica gel 60, chitosan, and the hybrid are shown in Figure 5 and their overlay in Figure 6; the main absorption bands and their assignments are listed in Table 2. Silica gel 60 showed the characteristic bands of the silica network, namely the strong asymmetric Si–O–Si stretching band at 1066.50 cm^{-1}, the Si–OH stretching band at 963.15 cm^{-1}, the symmetric Si–O–Si stretching band at about 799 cm^{-1}, and the Si–O–Si bending bands at 453.58–437.79 cm^{-1} [26]. Chitosan showed the broad O–H and N–H stretching band centered at about 3330 cm^{-1}, the C–H stretching band at 2877.96 cm^{-1}, the amide I (C=O stretching) band at 1649.27 cm^{-1}, the N–H bending band of the amino groups at 1587.54 cm^{-1}, the CH_2 bending and CH_3 deformation bands at 1418.17 and 1377.98 cm^{-1},



(a) (b) (c)

Figure 4. (a) Silica gel 60, (b) chitosan, and (c) chitosan–silica gel 60 hybrid.

Table 1. Summary of the purification of α-amylase from *A. fumigatus.*

Purification step	Volume (mL)	Unit activity ($U.mL^{-1}$)	Protein content ($mg.mL^{-1}$)	Specific activity ($U.mg^{-1}$)	Purification (fold)
Crude extract	1000	53.76	0.153	702.23	1
$(NH_4)_2SO_4$ fractionation (30–90)%	25	370.60	0.147	2520.91	3.6
Dialysis	60	124.57	0.036	3449.43	4.9

Table 2. Main FT-IR absorption bands (cm−1) of silica gel 60, chitosan, and the chitosan–silica gel 60 hybrid.

Assignment	Silica gel 60	Chitosan	Hybrid
O–H and N–H stretching (broad)	–	≈ 3330[a]	≈ 3320[a]
C–H stretching	–	2877.96	–
Amide I (C=O stretching); C=N (imine) in the hybrid	–	1649.27	1632.04
N–H bending ($–NH_2$); $–NH_3^+$ in the hybrid	–	1587.54	1538.74
CH_2 bending	–	1418.17	1426.78
CH_3 symmetric deformation	–	1377.98	–
Amide III (C–N stretching)	–	1317.69	–
C–O–C bridge stretching	–	1149.75	–
Si–O–Si asymmetric stretching; C–O stretching	1066.50	1065.06; 1024.87	1056.45
Si–OH stretching	963.15	–	971.76
ß-(1→4) pyranose ring	–	891.38	–
Si–O–Si symmetric stretching	≈ 799[a]	–	795.21
Si–O–Si bending	453.58; 444.97; 437.79	–	453.58; 446.41

–, band absent or not assigned. [a]Band not labeled by the instrument software; position read from the spectrum in Figure 5.

Copyright © 2027, ISSN 1978-2993

the amide III (C–N stretching) band at 1317.69 cm^{-1}, the C–O–C bridge stretching band at 1149.75 cm^{-1}, the C–O stretching bands at 1065.06 and 1024.87 cm^{-1}, and the band of the ß-(1→4)-linked pyranose ring at 891.38 cm^{-1} [31].

The hybrid spectrum combined the bands of both components (Table 2). The silica network was retained, as shown by the asymmetric and symmetric Si–O–Si stretching bands at 1056.45 and 795.21 cm^{-1} and the Si–O–Si bending bands at 453.58 and 446.41 cm^{-1}, whereas chitosan was identified by the bands at 1632.04, 1538.74, and 1426.78 cm^{-1}, together with the weak, broad O–H and N–H stretching band at 3266–3462 cm^{-1} (centered at about 3320 cm^{-1}). The weaker chitosan bands between 1380 and 890 cm^{-1} were not resolved in the hybrid, probably because they were masked by the intense Si–O–Si band. Likewise, the C–H stretching band of chitosan was obscured in the hybrid spectrum by weak inverted features at about 2984 and 2900 cm^{-1}; these features appear as small absorptions at 2984.18 and 2899.49 cm^{-1} in the silica gel 60 spectrum and were therefore attributed to the measurement background rather than to the samples. More importantly, the bands of the groups involved in the interaction between the two components were shifted. The amide I band of chitosan shifted from 1649.27 to 1632.04 cm^{-1}, which can be attributed to hydrogen bonding of the carbonyl groups and to the imine (C=N) bonds formed between the amino groups of chitosan and glutaraldehyde, which absorb in this region [32]. The N–H bending band shifted from 1587.54 to 1538.74 cm^{-1}, consistent with protonated amino groups ($–NH_3^+$) that interact electrostatically with deprotonated silanol groups ($Si–O^-$) and form hydrogen bonds with the silica surface [26,31]. On the silica side, the asymmetric Si–O–Si band shifted from 1066.50 to 1056.45 cm^{-1} and overlapped with the C–O and C–O–C bands of chitosan, which also explains its high intensity, and the Si–OH band shifted from 963.15 to 971.76 cm^{-1}, indicating that the silanol groups take part in hydrogen bonding with the hydroxyl and amino groups of chitosan [26].

These spectral features show that the hybrid is not a simple physical mixture of its components. Chitosan, cross-linked by glutaraldehyde, is bound to the surface of silica

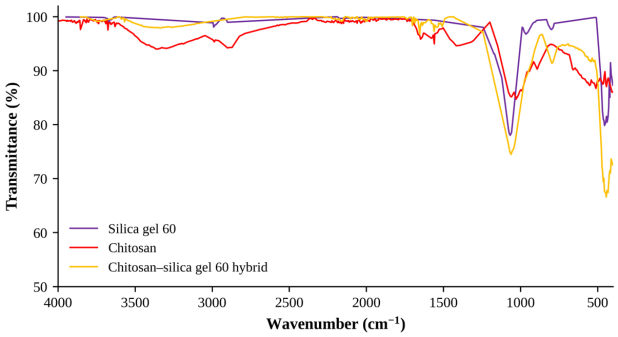


Figure 6. Overlay of the FT-IR spectra of silica gel 60, chitosan, and the chitosan–silica gel 60 hybrid.

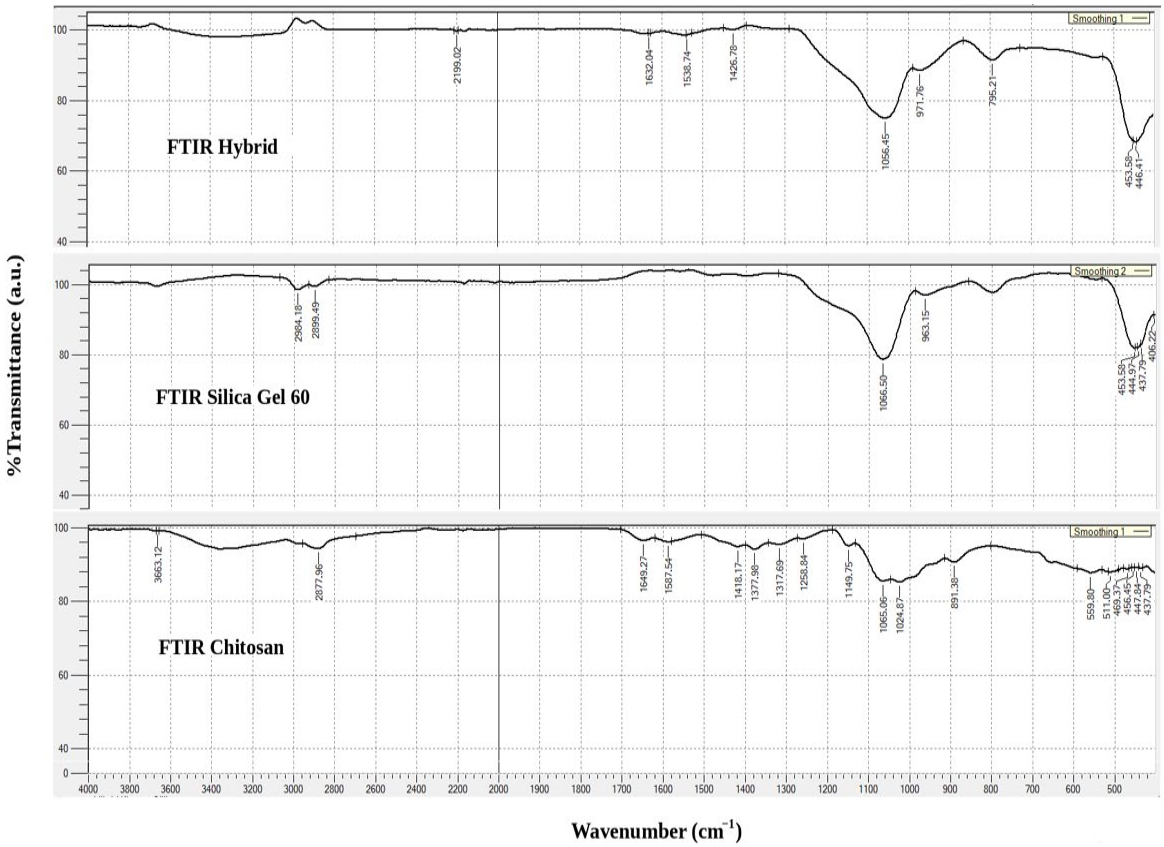


Figure 5. FT-IR spectra of silica gel 60, chitosan, and the chitosan–silica gel 60 hybrid.

Copyright © 2027, ISSN 1978-2993

gel 60 through hydrogen bonds and electrostatic interactions; that is, a chitosan–silica gel 60 hybrid was formed. This conclusion is supported by the different solubility of the hybrid, which, unlike chitosan, did not form a gel at pH of 4.0–4.5 (Section 3.5).

3.5. Enzyme–Matrix Binding Buffer pH

The interaction between the enzyme and the matrix in this immobilization is physical adsorption. The pH determines the strength of this interaction through electrostatic effects between charges on the enzyme and the matrix and through hydrogen bond formation [8]. The binding buffer pH was selected based on the highest activity of the immobilized enzyme, expressed relative to the highest activity (100%).

For silica gel 60, the highest activity was obtained at pH of 5 and decreased at higher pH (Figure 7); therefore, pH of 5 was used as the optimum binding condition. For chitosan, the highest activity was at pH of 4.5 (Figure 8). However, chitosan dissolved to form a gel at pH of 4 and 4.5, whereas an immobilization matrix must be insoluble in water to bind the enzyme effectively. The optimum binding pH for chitosan was therefore set at pH of 5. For the hybrid, the highest activity was at pH of 5.0 (Figure 9). Unlike chitosan, the hybrid did not form a gel at pH of 4 and 4.5, because hybridization with silica reduced the solubility of the material at relatively acidic pH.

All three matrices had acidic binding pH values. At these pH values, the enzyme is protonated, forming NH_3^+ groups on its side chains, which interact electrostatically with the partially negatively charged O atoms of the amide groups of chitosan and of silica gel (SiO_2). Hydrogen bonding between the enzyme and the matrix also plays a role [8].

Silanol groups on silica and amino/hydroxyl groups on chitosan can form covalent bonds with enzymes under activating conditions, but no such activation was applied here: silica gel 60 was used as supplied, without silanization or other surface functionalization, and residual glutaraldehyde was expected to have been removed by the repeated washing of the hybrid (Section 2.5) before the enzyme was introduced (Section 2.6). In the absence of an activating or coupling agent, the silanol, amino, and hydroxyl groups of the matrices can interact with the enzyme only through non-covalent electrostatic attraction and hydrogen bonding. This assignment is consistent with the strong pH dependence of binding (Figures 7–9) and with the gradual loss of activity on reuse (Section 3.10), both of which are typical of adsorption-based supports, whereas covalent attachment is generally less sensitive to pH and more resistant to leaching [13]. The enzyme–matrix interaction is therefore classified as physical adsorption; direct confirmation by quantifying enzyme leaching or by spectroscopic analysis of the enzyme-loaded matrices was not performed and is proposed as future work.

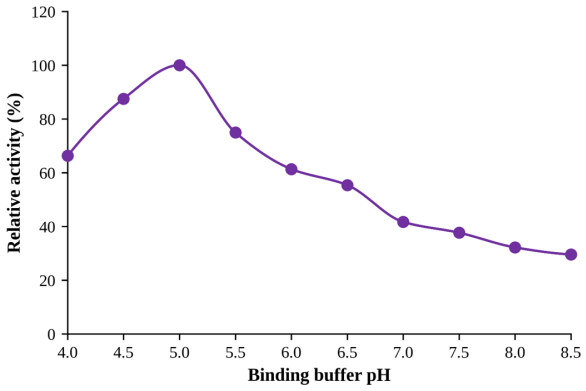


Figure 7. Activity of purified α-amylase on the silica gel 60 matrix at various binding buffer pH values.

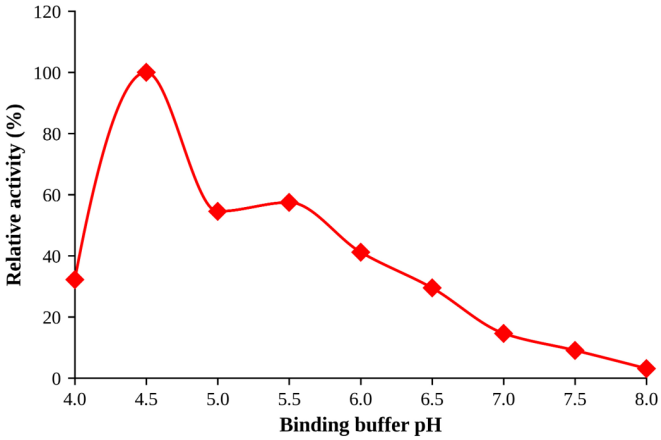


Figure 8. Activity of purified α-amylase on the chitosan matrix at various binding buffer pH values.

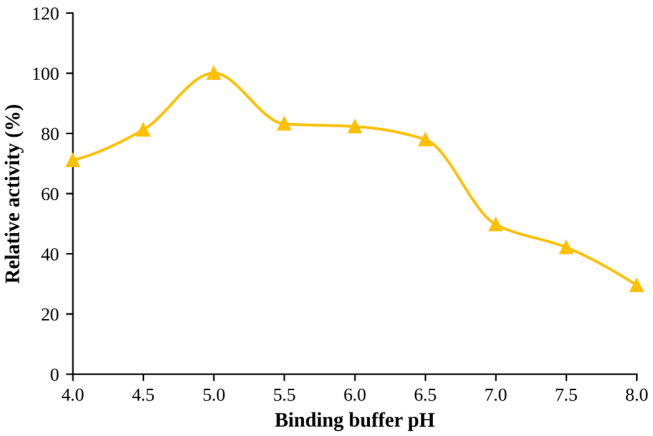


Figure 9. Activity of purified α-amylase on the chitosan–silica gel 60 hybrid matrix at various binding buffer pH values.

Copyright © 2027, ISSN 1978-2993

3.6. Optimum Temperature of the Purified and Immobilized Enzymes

The optimum temperature was determined from the highest relative activity of each sample (Figure 10). The purified enzyme had an optimum temperature of 50 °C, whereas the enzymes immobilized on silica gel 60, chitosan, and the hybrid had an optimum temperature of 55 °C. At higher temperatures, the activity of the purified enzyme decreased relatively more than that of the immobilized enzymes, so the immobilized enzymes retained higher catalytic activity at high temperatures. This improved thermostability is attributed to the adsorption of the enzyme on the matrix, which makes the enzyme relatively more rigid and less prone to conformational change [9,10]. An increase in the optimum temperature upon immobilization has also been reported for *A. fumigatus* α-amylase immobilized on chitin–bentonite [4] and for *Bacillus subtilis* α-amylase immobilized on chitosan–magnetic nanoparticles, whose optimum temperature increased by 10 °C [11].

3.7. Kinetic Parameters (K_M and V_{max})

The Michaelis–Menten constant (K_M) is the substrate concentration at which the reaction rate reaches half of V_{max} and reflects the apparent affinity of the enzyme for the substrate, whereas V_{max} is the maximum reaction rate at substrate saturation [28]. Both values were determined from Lineweaver–Burk plots (Figure 11) and are summarized in Table 3. The K_M values of all immobilized enzymes were higher than that of the purified enzyme, indicating a decrease in the apparent affinity of the enzyme for the substrate. This is attributed to non-covalent interactions between the enzyme and the matrix that can hinder substrate access to the active site. The V_{max} values of all immobilized enzymes were also lower than that of the purified enzyme, which can be attributed to conformational changes of the adsorbed enzyme and to steric and diffusional restrictions at the support surface [6,12].

These kinetic data indicate that the immobilized enzymes require a higher substrate concentration than the purified enzyme to reach half of their maximum rate. The enzyme–chitosan had the lowest V_{max} and the highest K_M, followed by the enzyme–hybrid, suggesting more extensive enzyme–matrix interaction on the chitosan-containing matrices than on silica gel 60 [33]. A similar increase in K_M and decrease in V_{max} were reported for α-amylase immobilized on a polyaniline magnetic nanocomposite [12], and an increase in K_M was also observed for α-amylase on chitosan–magnetic nanoparticles [11]. In contrast, adsorption of *A. fumigatus* α-amylase on bentonite/chitosan decreased K_M and increased V_{max} [19], showing that the effect of immobilization on the apparent kinetic parameters depends strongly on the support. Because these parameters are apparent values, they also include the effect of substrate diffusion to the enzyme bound on the support particles [6].

The higher apparent K_M of the immobilized enzymes and the higher substrate concentration they require are linked mechanistically. When

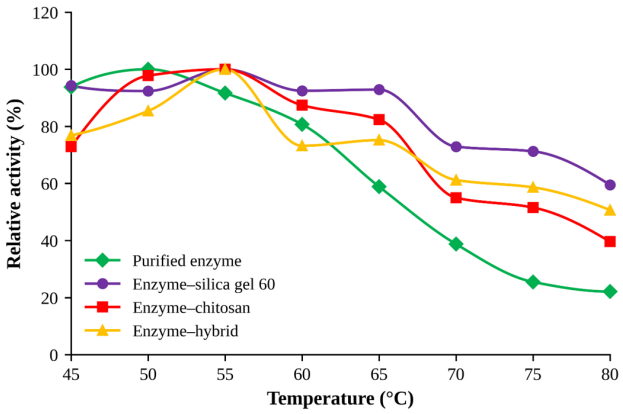


Figure 10. Optimum temperature of purified α-amylase and α-amylase immobilized on silica gel 60, chitosan, and the chitosan–silica gel 60 hybrid.

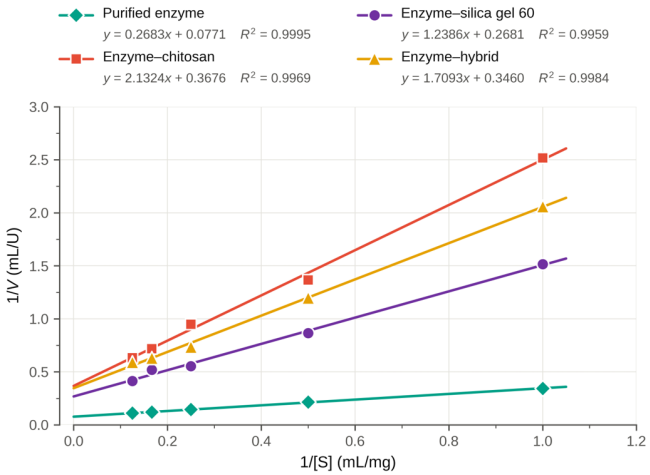


Figure 11. Lineweaver–Burk plots of purified α-amylase and α-amylase immobilized on silica gel 60, chitosan, and the chitosan–silica gel 60 hybrid. Lines are linear regressions; their equations and R^2 values are given above the plot.

Table 3. K_M and V_{max} values of purified α-amylase and α-amylase immobilized on silica gel 60, chitosan, and the chitosan–silica gel 60 hybrid.

Sample	V_{max} (μmol.mL^{-1}.min^{-1})	K_M (mg.mL^{-1})
Purified enzyme	12.97	3.48
Enzyme–silica gel 60	3.73	4.62
Enzyme–chitosan	2.72	5.80
Enzyme–hybrid	2.89	4.94

Copyright © 2027, ISSN 1978-2993

the enzyme is adsorbed in a fixed orientation and is partly embedded in the matrix surface, access of the substrate to the active site is sterically restricted and depends on diffusion through the stagnant layer around the support particles [6]. A higher bulk substrate concentration is therefore needed to maintain the concentration gradient, and thus the degree of active-site saturation, that the freely diffusing purified enzyme reaches at a lower concentration. Consistent with this interpretation, the increase in apparent K_M was smallest for enzyme–silica gel 60 and largest for enzyme–chitosan (Table 3). Diffusional and conformational contributions cannot be separated with the present data, because the apparent parameters were not corrected for mass-transfer limitations.

The consequence of these kinetic changes for conversion was evaluated from the parameters in Tables 3 and 4 and from the reusability data (Section 3.10) (Table 5), assuming equal enzyme input for all preparations and 30 min per reaction cycle. The catalytic efficiency (V_{max}/K_M) of the immobilized enzymes was only 13–22% of that of the purified enzyme, and their initial rates at the highest starch concentration tested (8 mg.mL^{-1}) were 17–26% of that of the purified enzyme. Over six reuse cycles, the cumulative product of enzyme–hybrid (1.02) and enzyme–silica gel 60 (1.06) was about equal to that of a single use of the purified enzyme, and that of enzyme–chitosan was lower (0.68). In a batch held at 60 °C, with first-order inactivation, the purified enzyme gave more product than any immobilized preparation during the first hours, and the enzyme–hybrid overtook it only after about 7 h (437 min). Under the conditions tested, the improved stability of the immobilized enzyme therefore does not by itself translate into higher productivity per unit of enzyme. Its benefits lie in recovery of the biocatalyst, in operation over more cycles than the six tested (57% of the initial activity was retained by the hybrid), and in the absence of enzyme in the product stream, which are the process benefits that usually justify the cost of immobilization [34]. Because the enzyme loading, the immobilization yield, the cost of the support, and operation in a repeated-batch or continuous reactor were not determined, a techno-economic evaluation cannot be made from the present data and is recommended as future work.

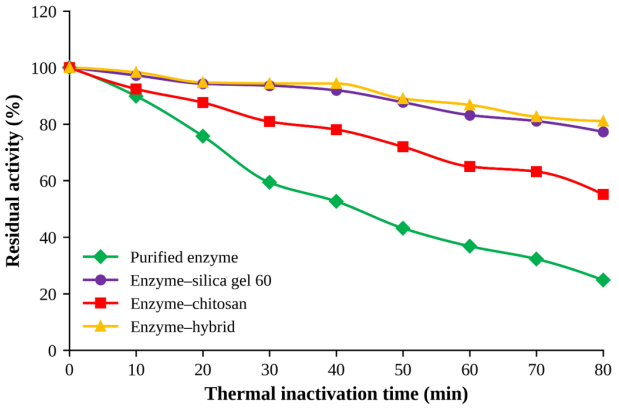


Figure 12. Thermal stability (60 °C, 80 min) of purified α-amylase and α-amylase immobilized on silica gel 60, chitosan, and the chitosan–silica gel 60 hybrid.

3.8. Thermal Stability

Thermal stability was determined from the residual activity after inactivation at 60 °C for 80 min (Figure 12). The residual activity of the purified enzyme was 24.8%, whereas those of the enzymes immobilized on silica gel 60, chitosan, and the hybrid were 77.3, 55.1, and 81.1%, respectively. All immobilized enzymes were thus more heat-stable than the purified enzyme, owing to the conformational resistance of the enzyme bound non-covalently to the matrix, which makes it difficult to denature [8,10]. The enzyme–hybrid showed the highest residual activity, supporting the suggestion that the interaction of the enzyme with the hybrid matrix is stronger and more rigid than with the other matrices. This residual activity was also higher than the 59.61% reported for *A. fumigatus* α-amylase immobilized on bentonite/chitosan under the same inactivation conditions (60 °C, 80 min) [19].

3.9. Thermal Inactivation Rate Constant, Half-Life, and Free Energy Change of Inactivation

The k_i values were obtained from the slopes of $\ln(E_i/E_0)$ versus inactivation time according to first-order kinetics (Figure 13) and were then

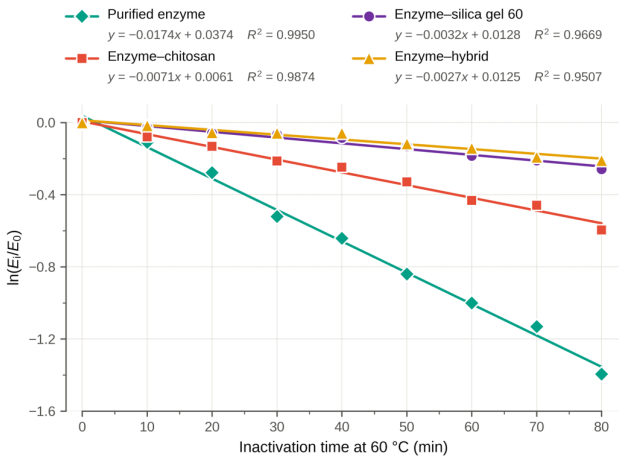


Figure 13. First-order thermal inactivation plots (60 °C) of purified α-amylase and α-amylase immobilized on silica gel 60, chitosan, and the chitosan–silica gel 60 hybrid. Lines are linear regressions; their equations and R² values are given above the plot.

Copyright © 2027, ISSN 1978-2993

used to calculate $t_{1/2}$ and ΔG_i (Table 4). The k_i of the enzyme–hybrid (2.657×10^{-3} min^{-1}) was the lowest compared with the purified enzyme (17.36×10^{-3} min^{-1}), enzyme–silica gel 60 (3.153×10^{-3} min^{-1}), and enzyme–chitosan (7.060×10^{-3} min^{-1}), so the enzyme–hybrid was denatured most slowly. This is probably due to the increased rigidity resulting from the interaction of the enzyme with the matrix, which strengthens the tertiary structure of the enzyme [10,18].

All immobilized enzymes had higher $t_{1/2}$ and ΔG_i values than the purified enzyme. A higher $t_{1/2}$ means that the immobilized enzyme takes longer to lose its activity, and a higher ΔG_i means that more energy is required to denature it [10,18]. The enzyme–hybrid showed the greatest stability increase, 6.5-fold relative to the purified enzyme, with a $t_{1/2}$ of 260.85 min and a ΔG_i of 109.62 kJ.mol^{-1}. This stability increase is higher than the 4.44-fold increase reported for *A. fumigatus* α-amylase immobilized on bentonite/chitosan at the same temperature [19]. This result supports the view that the enzyme interacts more extensively with the hybrid matrix than with silica gel 60 or chitosan alone.

3.10. Reusability

Reusability is an advantage of immobilized enzymes over free enzymes, because the purified enzyme cannot be separated after the enzymatic reaction is complete. After the sixth use, the residual activities of the enzymes immobilized on silica gel 60, chitosan, and the hybrid were 44, 25, and 57%, respectively (Figure 14). The enzyme–hybrid gave the highest residual activity, which is attributed to the mutually reinforcing effect of silica gel 60 and chitosan in the hybrid, keeping the enzyme bound and active compared with silica gel 60 or chitosan alone. This value is also higher than the 47.61% retained by *A. fumigatus* α-amylase on bentonite/chitosan after six cycles [19]. The gradual loss of activity during reuse may be partly caused by desorption of the physically adsorbed enzyme during washing, a known limitation of adsorption-based immobilization [13]; covalent attachment, as on glutaraldehyde-activated chitosan–magnetic nanoparticles that retained 83.2% of the initial activity after 15 cycles [11], may further improve the operational stability.

Comparison with commercially available immobilized α-amylase is limited, because few immobilized-enzyme processes have been

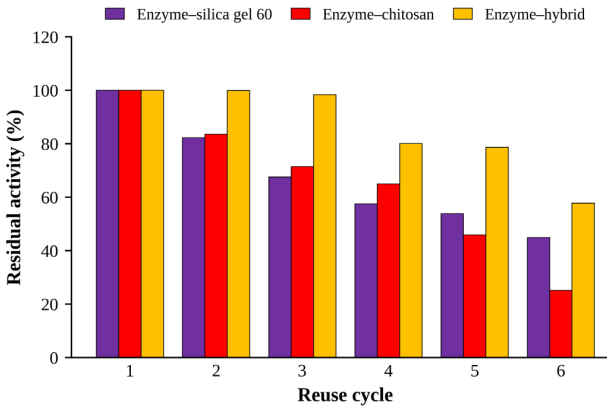


Figure 14. Reusability of α-amylase immobilized on silica gel 60, chitosan, and the chitosan–silica gel 60 hybrid.

Table 4. k_i, $t_{1/2}$, and ΔG_i values of purified α-amylase and α-amylase immobilized on silica gel 60, chitosan, and the chitosan–silica gel 60 hybrid.

Sample	k_i ($\times 10^{-3}$ min^{-1})	$t_{1/2}$ (min)	ΔG_i (kJ.mol^{-1})	Stability increase (fold)
Purified enzyme	17.36	39.93	104.43	1
Enzyme–silica gel 60	3.153	219.81	109.15	5.5
Enzyme–chitosan	7.060	98.18	106.92	2.5
Enzyme–hybrid	2.657	260.85	109.62	6.5

Table 5. Productivity indicators of purified α-amylase and α-amylase immobilized on silica gel 60, chitosan, and the chitosan–silica gel 60 hybrid, calculated from Tables 3 and 4 and Figure 14.

Sample	V_{max}/K_M (% of purified)	Initial rate at 8 mg.mL^{-1} (% of purified)	Product over six reuse cycles[a]	Product in 80 min at 60 °C[b]
Purified enzyme	100	100	1.00 (single use)	1.00
Enzyme–silica gel 60	22	26	1.06	0.47
Enzyme–chitosan	13	17	0.68	0.30
Enzyme–hybrid	16	20	1.02	0.37

Note: Values are relative to a single use of the purified enzyme and assume equal enzyme input and 30 min per cycle. Initial rates were calculated with the Michaelis–Menten equation using the V_{max} and K_M in Table 3. [a]Initial rate × sum of the relative residual activities of cycles 1–6 in Figure 14 (read from the figure). [b]$V_{max}[1 - \exp(-k_i\, t)]/k_i$ for t = 80 min, with k_i from Table 4 (first-order inactivation).

Copyright © 2027, ISSN 1978-2993

commercialized and the added cost of immobilization is difficult to justify unless process benefits are obtained [34]; no commercial immobilized α-amylase preparation with published thermal inactivation and reuse data under comparable conditions could be identified. The results were therefore compared with immobilized α-amylases from other sources (Table 6): a commercial porcine pancreatic α-amylase (Sigma-Aldrich) immobilized by ionic cross-linking in a gellan hydrogel, which showed an increase in optimum temperature from 35 to 60 °C and retained about 75% of its activity after 10 cycles and about 28% after 15 cycles [35], and *Bacillus subtilis* α-amylase covalently attached to chitosan–magnetic nanoparticles, which retained 83.2% after 15 cycles [11]. Relative to the supports previously tested for *A. fumigatus* α-amylase, the chitosan–silica gel 60 hybrid retained more activity after six cycles (57%) than the bentonite/chitosan [19], chitin–bentonite [4], bentonite [10], and zeolite/chitosan [18] supports (47.61, 38, 42, and 10.97% after six, six, six, and five cycles, respectively). Because the number of cycles and the conditions differ among these studies, the comparison is indicative only; covalent attachment retained more activity over more cycles [11], which is consistent with the adsorption mechanism assigned in Section 3.5.

4. Conclusions

α-Amylase from *A. fumigatus* was purified 4.9-fold (3449.43 U.mg^{-1}) by (30–90)% ammonium sulfate fractionation and dialysis. FT-IR analysis confirmed the formation of the chitosan–silica gel 60 hybrid, which showed the bands of both components together with shifts of the amide I, N–H, Si–O–Si, and Si–OH bands. The enzyme was immobilized by physical adsorption on silica gel 60, chitosan, and the hybrid at a binding pH of 5.0. Immobilization raised the optimum temperature from 50 to 55 °C, increased K_M, and decreased V_{max}. The enzyme–hybrid had the highest thermal stability, with 81.1% residual activity after 80 min at 60 °C, a $t_{1/2}$ of 260.85 min, and a 6.5-fold stability increase, as well as the highest residual activity (57%) after six uses. These results show that hybridizing chitosan with silica gel 60 yields a more stable and reusable α-amylase biocatalyst than either component alone, while avoiding the gel formation of chitosan at acidic pH. Future work should quantify enzyme leaching from the hybrid, examine covalent attachment of the enzyme to the hybrid, and evaluate the immobilized enzyme in continuous starch hydrolysis. The improved stability was accompanied by a lower catalytic efficiency (13–22% of that of the purified enzyme), so the net productivity gain depends on reuse and on long-duration operation. Future work should also determine the enzyme loading and immobilization yield, quantify productivity and economics in repeated-batch operation, and include a cross-linker-free hybrid as a synthesis control.

Acknowledgements

The authors are grateful to the Ministry of Education, Culture, Research and Technology (Indonesia) for funding this study through the 2023 Basic Research scheme (contract numbers 027/E5/PG.02.00.PL/2023, dated 12 April 2023, and 2192/UN26.21/PN/2023, dated 17 April 2023).

Table 6. Stability and reusability of α-amylase immobilized on the chitosan–silica gel 60 hybrid compared with previously reported immobilized α-amylases.

Support	Enzyme source	Half-life increase (fold)	Residual activity after reuse	Ref.
Chitosan–silica gel 60 hybrid (this work)	*A. fumigatus*	6.5	57% (6 cycles)	–
Silica gel 60 (this work)	*A. fumigatus*	5.5	44% (6 cycles)	–
Chitosan (this work)	*A. fumigatus*	2.5	25% (6 cycles)	–
Bentonite/chitosan	*A. fumigatus*	4.44	47.61% (6 cycles)	[19]
Zeolite/chitosan	*A. fumigatus*	4.65	10.97% (5 cycles)	[18]
Chitin–bentonite	*A. fumigatus*	3.80[a]	38% (6 cycles)	[4]
Bentonite	*A. fumigatus*	2.85[a]	42% (6 cycles)	[10]
Chitosan–magnetic nanoparticles (covalent)	*B. subtilis* MK1	n.r.	83.2% (15 cycles)	[11]
Gellan hydrogel (ionic cross-linking)	Porcine pancreas (commercial)[b]	n.r.	≈75% (10 cycles); ≈28% (15 cycles)	[35]

Note: n.r., not reported. [a]Calculated from the reported half-lives of the immobilized enzymes (154.00 and 115.50 min) and of the free enzyme (40.53 min). [b]Enzyme purchased from Sigma-Aldrich.

Copyright © 2027, ISSN 1978-2993

Conflict of Interest Statement

The authors declare that they have no known competing financial interests or personal relationships that could have appeared to influence the work reported in this paper.

Declaration of Generative AI Use

During the revision of this manuscript, the authors used Claude (Anthropic) to assist in drafting the revised text, the comparison with the literature, the response to the reviewers' comments, and the layout of the graphical abstract. After using this tool, the authors reviewed and edited the content as needed and take full responsibility for the content of the publication. Generative AI was not used to generate or alter the experimental data or the figures that report experimental results.

CRediT Author Statement

Author Contributions: S. Alba: Conceptualization, Formal Analysis, Investigation, Writing – Original Draft; Y. Yandri: Conceptualization, Funding Acquisition, Methodology, Supervision, Writing – Review & Editing; T. Suhartati: Methodology, Supervision, Writing – Review & Editing; B. Irawan: Methodology, Resources, Writing – Review & Editing; S. Waruwu: Formal Analysis, Investigation, Writing – Review & Editing. All authors have read and agreed to the published version of the manuscript.

References

[1] Gupta, R., Gigras, P., Mohapatra, H., Goswami, V.K., Chauhan, B. (2003). Microbial α-amylases: A biotechnological perspective. *Process Biochemistry*, 38(11), 1599–1616. DOI: 10.1016/S0032-9592(03)00053-0.

[2] Jujjavarapu, S.E., Dhagat, S. (2019). Evolutionary trends in industrial production of α-amylase. *Recent Patents on Biotechnology*, 13(1), 4–18. DOI: 10.2174/2211550107666180816093436.

[3] Nwagu, T.N., Okolo, B.N. (2011). Growth profile and amylolytic activity of a thermophilic fungus *Aspergillus fumigatus* isolated from soil. *Asian Journal of Biotechnology*, 3(1), 46–57. DOI: 10.3923/ajbkr.2011.46.57.

[4] Tiarsa, E.R., Yandri, Y., Suhartati, T., Satria, H., Irawan, B., Hadi, S. (2022). The stability improvement of *Aspergillus fumigatus* α-amylase by immobilization onto chitin-bentonite hybrid. *Biochemistry Research International*, 2022, 5692438. DOI: 10.1155/2022/5692438.

[5] Sheldon, R.A., van Pelt, S. (2013). Enzyme immobilisation in biocatalysis: Why, what and how. *Chemical Society Reviews*, 42(15), 6223–6235. DOI: 10.1039/C3CS60075K.

[6] Liese, A., Hilterhaus, L. (2013). Evaluation of immobilized enzymes for industrial applications. *Chemical Society Reviews*, 42(15), 6236–6249. DOI: 10.1039/C3CS35511J.

[7] Mateo, C., Palomo, J.M., Fernandez-Lorente, G., Guisan, J.M., Fernandez-Lafuente, R. (2007). Improvement of enzyme activity, stability and selectivity via immobilization techniques. *Enzyme and Microbial Technology*, 40(6), 1451–1463. DOI: 10.1016/j.enzmictec.2007.01.018.

[8] Maghraby, Y.R., El-Shabasy, R.M., Ibrahim, A.H., Azzazy, H.M.E. (2023). Enzyme immobilization technologies and industrial applications. *ACS Omega*, 8(6), 5184–5196. DOI: 10.1021/acsomega.2c07560.

[9] Bindu, V.U., Mohanan, P.V. (2017). Enhanced stability of α-amylase via immobilization onto chitosan-TiO_2 nanocomposite. *Nanoscience & Technology: Open Access*, 4(2), 1–9. DOI: 10.15226/2374-8141/4/2/00146.

[10] Yandri, Y., Tiarsa, E.R., Suhartati, T., Satria, H., Irawan, B., Hadi, S. (2022). The stability improvement of α-amylase enzyme from *Aspergillus fumigatus* by immobilization on a bentonite matrix. *Biochemistry Research International*, 2022, 3797629. DOI: 10.1155/2022/3797629.

[11] Ahmed, S.A., Abdella, M.A.A., El-Sherbiny, G.M., Ibrahim, A.M., El-Shamy, A.R., Atalla, S.M.M., Hassan, M.E. (2020). Catalytic, kinetic and thermal properties of free and immobilized *Bacillus subtilis*-MK1 α-amylase on chitosan-magnetic nanoparticles. *Biotechnology Reports*, 26, e00443. DOI: 10.1016/j.btre.2020.e00443.

[12] Augustine, M., Madhusudhanan, D.T., Velayudhan, M.P. (2023). Thermal deactivation studies of alpha-amylase immobilized onto core-shell structured aniline formaldehyde crosslinked polyaniline magnetic nanocomposite. *Biotechnology & Biotechnological Equipment*, 37(1), 273–285. DOI: 10.1080/13102818.2023.2182150.

[13] Hartmann, M., Kostrov, X. (2013). Immobilization of enzymes on porous silicas – Benefits and challenges. *Chemical Society Reviews*, 42(15), 6277–6289. DOI: 10.1039/C3CS60021A.

[14] Agustian, J., Hermida, L. (2025). Salt-assisted mesostructured cellular foam (MCF) silica synthesis from bagasse bottom ash for enzymatic starch hydrolysis. *Bulletin of Chemical Reaction Engineering & Catalysis*, 20(3), 428–440. DOI: 10.9767/bcrec.20379.

[15] Krajewska, B. (2004). Application of chitin- and chitosan-based materials for enzyme immobilizations: A review. *Enzyme and Microbial Technology*, 35(2–3), 126–139. DOI: 10.1016/j.enzmictec.2003.12.013.

[16] Girelli, A.M., Quattrocchi, L., Scuto, F.R. (2020). Silica-chitosan hybrid support for laccase immobilization. *Journal of Biotechnology*, 318, 45–50. DOI: 10.1016/j.jbiotec.2020.05.004.

Copyright © 2027, ISSN 1978-2993

[17] Cahyaningrum, S.E., Sianita, M.M. (2014). Immobilization of pepsin onto chitosan silica nanobeads with glutaraldehyde as crosslink agent. *Bulletin of Chemical Reaction Engineering & Catalysis*, 9(3), 263–269. DOI: 10.9767/bcrec.9.3.7060.263-269.

[18] Yandri, Y., Ropingi, H., Suhartati, T., Hendri, J., Irawan, B., Hadi, S. (2022). The effect of zeolite/chitosan hybrid matrix for thermal-stabilization enhancement on the immobilization of *Aspergillus fumigatus* α-amylase. *Emerging Science Journal*, 6(3), 505–518. DOI: 10.28991/ESJ-2022-06-03-06.

[19] Yandri, Y., Ropingi, H., Suhartati, T., Irawan, B., Hadi, S. (2023). Immobilization of *Aspergillus fumigatus* α-amylase via adsorption onto bentonite/chitosan for stability enhancement. *Emerging Science Journal*, 7(5), 1811–1826. DOI: 10.28991/ESJ-2023-07-05-023.

[20] Deb, P., Talukdar, S.A., Mohsina, K., Sarker, P.K., Sayem, S.M.A. (2013). Production and partial characterization of extracellular amylase enzyme from *Bacillus amyloliquefaciens* P-001. *SpringerPlus*, 2, 154. DOI: 10.1186/2193-1801-2-154.

[21] Bollag, D.M., Rozycki, M.D., Edelstein, S.J. (1996). *Protein Methods*. 2nd Edition. New York: Wiley-Liss.

[22] Fuwa, H. (1954). A new method for microdetermination of amylase activity by the use of amylose as the substrate. *The Journal of Biochemistry*, 41(5), 583–603. DOI: 10.1093/oxfordjournals.jbchem.a126476.

[23] Eveleigh, D.E., Mandels, M., Andreotti, R., Roche, C. (2009). Measurement of saccharifying cellulase. *Biotechnology for Biofuels*, 2, 21. DOI: 10.1186/1754-6834-2-21.

[24] Lowry, O.H., Rosebrough, N.J., Farr, A.L., Randall, R.J. (1951). Protein measurement with the Folin phenol reagent. *Journal of Biological Chemistry*, 193(1), 265–275. DOI: 10.1016/S0021-9258(19)52451-6.

[25] Baysal, Z., Bulut, Y., Yavuz, M., Aytekin, Ç. (2014). Immobilization of α-amylase via adsorption onto bentonite/chitosan composite: Determination of equilibrium, kinetics, and thermodynamic parameters. *Starch/Stärke*, 66(5–6), 484–490. DOI: 10.1002/star.201300133.

[26] Budnyak, T.M., Pylypchuk, I.V., Tertykh, V.A., Yanovska, E.S., Kolodynska, D. (2015). Synthesis and adsorption properties of chitosan-silica nanocomposite prepared by sol-gel method. *Nanoscale Research Letters*, 10, 87. DOI: 10.1186/s11671-014-0722-1.

[27] Ghiaci, M., Aghaei, H., Soleimanian, S., Sedaghat, M.E. (2009). Enzyme immobilization: Part 1. Modified bentonite as a new and efficient support for immobilization of *Candida rugosa* lipase. *Applied Clay Science*, 43(3–4), 289–295. DOI: 10.1016/j.clay.2008.09.008.

[28] Robinson, P.K. (2015). Enzymes: Principles and biotechnological applications. *Essays in Biochemistry*, 59, 1–41. DOI: 10.1042/bse0590001.

[29] Duong-Ly, K.C., Gabelli, S.B. (2014). Salting out of proteins using ammonium sulfate precipitation. *Methods in Enzymology*, 541, 85–94. DOI: 10.1016/B978-0-12-420119-4.00007-0.

[30] Virgen-Ortíz, J.J., Ibarra-Junquera, V., Osuna-Castro, J.A., Escalante-Minakata, P., Mancilla-Margalli, N.A., Ornelas-Paz, J. de J. (2012). Method to concentrate protein solutions based on dialysis–freezing–centrifugation: Enzyme applications. *Analytical Biochemistry*, 426(1), 4–12. DOI: 10.1016/j.ab.2012.03.019.

[31] Kumirska, J., Czerwicka, M., Kaczyński, Z., Bychowska, A., Brzozowski, K., Thöming, J., Stepnowski, P. (2010). Application of spectroscopic methods for structural analysis of chitin and chitosan. *Marine Drugs*, 8(5), 1567–1636. DOI: 10.3390/md8051567.

[32] Monteiro, O.A.C., Airoldi, C. (1999). Some studies of crosslinking chitosan–glutaraldehyde interaction in a homogeneous system. *International Journal of Biological Macromolecules*, 26(2–3), 119–128. DOI: 10.1016/S0141-8130(99)00068-9.

[33] Califano, V., Costantini, A. (2020). Immobilization of cellulolytic enzymes in mesostructured silica materials. *Catalysts*, 10(6), 706. DOI: 10.3390/catal10060706.

[34] DiCosimo, R., McAuliffe, J., Poulose, A.J., Bohlmann, G. (2013). Industrial use of immobilized enzymes. *Chemical Society Reviews*, 42(15), 6437–6474. DOI: 10.1039/C3CS35506C.

[35] Tincu (Iurciuc), C.E., Bouhadiba, B., Atanase, L.I., Stan, C.S., Popa, M., Ochiuz, L. (2023). An accessible method to improve the stability and reusability of porcine pancreatic α-amylase via immobilization in gellan-based hydrogel particles obtained by ionic cross-linking with Mg^{2+} ions. *Molecules*, 28(12), 4695. DOI: 10.3390/molecules28124695.

Copyright © 2027, ISSN 1978-2993